JOURNAL OF MATERIALS SCIENCE **34** (1999) 5661–5668

Microstructural evolution and its relation to mechanical properties in a drawn dual-phase steel

WON JONG NAM, CHUL MIN BAE
POSCO Technical Research Lab., Pohang 790-785, Korea

Microstructural changes and their relations to mechanical properties in drawn dual-phase steels were investigated by performing tensile tests and microstructural examination with scanning electron microscopy. In this investigation, the primary focus was on deformation behavior of martensite particles aligned transverse to the drawing axis. Unlike martensite particles aligned nearly parallel to the drawing axis that are thinned to a fibrous shape, those aligned transverse to the drawing axis are severely bent, and even fractured with increasing drawing strain. In addition, the realignment of martensite particles to the drawing axis is directly related to the occurrence of a maximum peak in RA, of an inflection point in tensile strength and of a sharp drop in work hardening rate. The variation of mechanical properties of reduction in area, tensile strength and work hardening rate with drawing strain is discussed in conjunction with microstructural changes during the drawing.

1. Introduction

It is well known that the low carbon dual-phase steels developed in the past decades offer low yield strength, continuous yielding, high work hardening rate, good formability and good ductility [1–3]. Among various properties, high work hardening rate and good ductility make dual phase steels very attractive for use in cold drawn high strength steel wires, since they lead to higher strength and better drawability.

A number of investigations concerning work hardening behavior in conjunction with microstructural factors such as the composition, size, distribution and volume fraction of martensite produced by composition and heat treatment modifications, have been reported [4–9]. Unlike most steels, the work hardening processes in dual-phase steels under uniaxial tension are complex. The work hardening behavior under uniaxial tension can be divided into three strain regions, and each region shows a different work hardening rate. Cribb and Rigsbee [4] have analyzed three-stage behavior in terms of deformation mechanisms correlated with microstructure. The rapid work hardening in the first stage represents the elimination of residual stresses and the rapid buildup of back stress in the ferrite caused by the plastic instability of the two phases. In the second stage, the decrease of work hardening rate is attenuated due to the constrained deformation of the ferrite caused by the presence of rigid martensite. In the third stage, the formation of dislocation cell structures begins, and further deformation in the ferrite is governed by dynamic recovery and cross-slip and by eventual yielding of the martensite phase. However, the strain range in previous work has been limited to less than 0.2 true strain in uniaxial tension. Little information is available about whether work hardening behavior observed in uniaxial tension is valid when the deformation method is changed to wire drawing with relatively large strain. It is, therefore, of interest to investigate work hardening behavior of dual-phase steel wires drawn to high strains.

More significantly, the ductility of a dual-phase steel wire is influenced by the morphology and distribution of martensite. Sidjanin and Miyasato [10] have shown that the initiation of voids, during wire drawing, occurs by the decohesion of ferrite/martensite interfaces or by the shear cracking of martensite particles. However, Nakagawa and Thomas [11] and Szewczyk and Gurland [12] have observed that the majority of voids is formed at the ferrite/martensite interface rather than the cracked martensite, and eventually coalesce to cause failure during subsequent tensile loading or drawing. Thus, it is important that the martensite produced by heat treatments must be kept as deformable as possible to remain coherent with the ferrite matrix during cold deformation. Among the various martensite morphologies produced by heat treatment, the fibrous lath martensite, with a high degree of initial structural coherency with the surrounding ferrite, leads to the least void density and the highest drawing limit [10, 13]. Nevertheless, the deformation behavior of martensite particles and its influence on mechanical properties in the intermediate strain range (0.5–6.0 true strain) during drawing have not been clarified yet, since most previous works has been concentrated on the failure mechanisms, such as void formation and/or fracture of martensite, operating during drawing of dual-phase steel wires. It would

be, therefore, worth investigating the transition from initially randomly distributed martensite particles to martensite fibers aligned parallel to the drawing direction, and its relation to the variations of reduction in area (RA) and tensile strength (TS) during drawing deformation.

Accordingly, in this study, it is attempted to investigate microstructural changes in the intermediate strain range during wire drawing and their relationship to mechanical properties such as RA and TS. More significantly, the work hardening behavior in conjunction with the deformation behavior of martensite particles is described.

2. Experimental

The material used in this study was the low carbon steel with chemical composition of 0.06%C-0.88%Si-1.5%Mn (in weight). The steel was received as a form of wire rod with an initial diameter of 5.5 mm. Among the various heat treatments [10, 12, 13], the intermediate quenching treatment, which was known to show the least void density and the highest drawing limit, was chosen. Samples were austenitized at 1000 °C for 15 min, and quenched in water, intercritically annealed at the temperatures of 820 °C (steel A) and 850 °C (steel B) for 10 min, and then quenched in water again.

To remove decarburized layers, heat treated specimens were machined to 5.0 mm dia. The rods were cold drawn on a single-head draw bench at the relatively low drawing speed of 10 m/min. Reduction of area in each pass was about 15% and the resultant final diameter was 0.09 mm, which was equivalent to true strain, ε, of about 8.0 ($\varepsilon = In\,(A_o/A)$, where A_o is the original cross-sectional area of the wire rod and A is the cross-sectional area of the drawn wire).

After each pass during the drawing operation, samples were taken for tensile testing and the observation of microstructures. Tensile tests were performed at an initial strain rate of $8.3 \times 10^{-4}\,s^{-1}$ on an Instron machine. The reported values of the mechanical data were the average of those obtained from at least three tests performed under identical conditions. The observation of microstructures was made on the sections parallel to the drawing axis, using a scanning electron microscope (SEM) after conventional mechanical polishing followed by etching in Le Pera's reagent [14]. The measurement of volume fraction of martensite was carried out by conventional point-counting on SEM micrographs (×2000 magnification). The values, Table I, were the average of those obtained from at least 10 SEM micrographs for each sample.

TABLE I Martensite volume fractions

	Annealing temperature (°C)	Volume fraction of martensite (%)	Carbon in martensite (%)[a]
Steel A	820	35.7	0.16
Steel B	850	43.6	0.14

[a] Estimated from the volume fraction and bulk carbon content.

3. Results and discussion

3.1. Microstructural evolution during drawing

The as-heat treated microstructure and the volume fraction of martensite are given in Fig. 1 and Table I, respectively. A fine fibrous distribution of martensite particles in the ferrite matrix (Fig. 1), indicates that the initial microstructure before annealing was martensite. Upon annealing in the two-phase region, the austenite nucleates and grows preferentially along the lath and packet boundaries of martensite, and then transforms to fine fibrous martensite particles upon quenching [15].

Fig. 2 shows how martensite particles which have an initially random orientation become progressively aligned along the drawing axis with the increase of drawing strain. The deformation behavior of martensite particles which are aligned nearly transverse to the drawing axis is quite different from that of favorably oriented martensite particles. At a strain of 0.93 (Fig. 2a), martensite particles aligned transverse to the drawing axis (marked A) are bent or even fractured to change their orientation to the drawing axis, while those aligned nearly parallel to the drawing axis (marked B) are plastically deformed, i.e., thinned and necked at

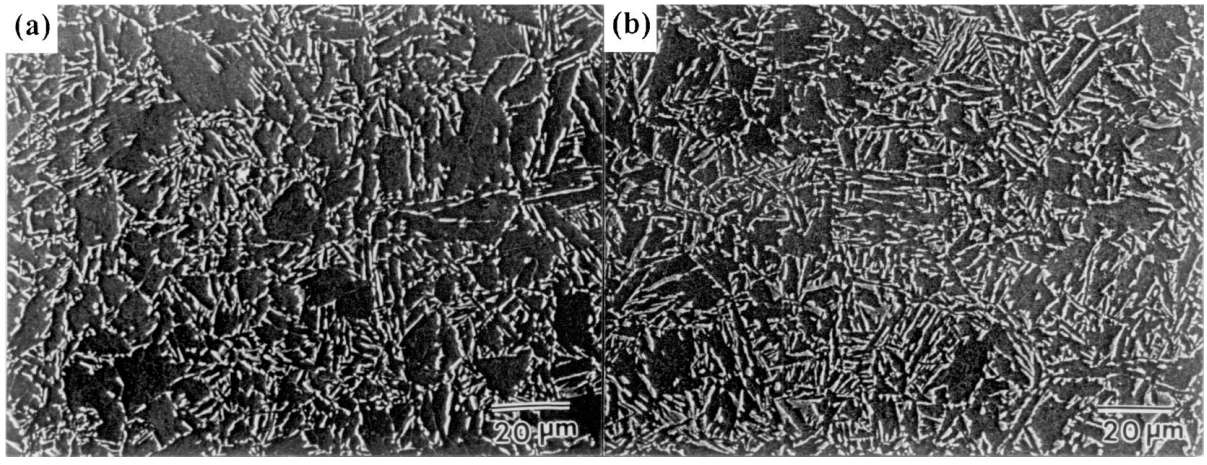

Figure 1 As-heat treated microstructures: (a) steel A; (b) steel B.

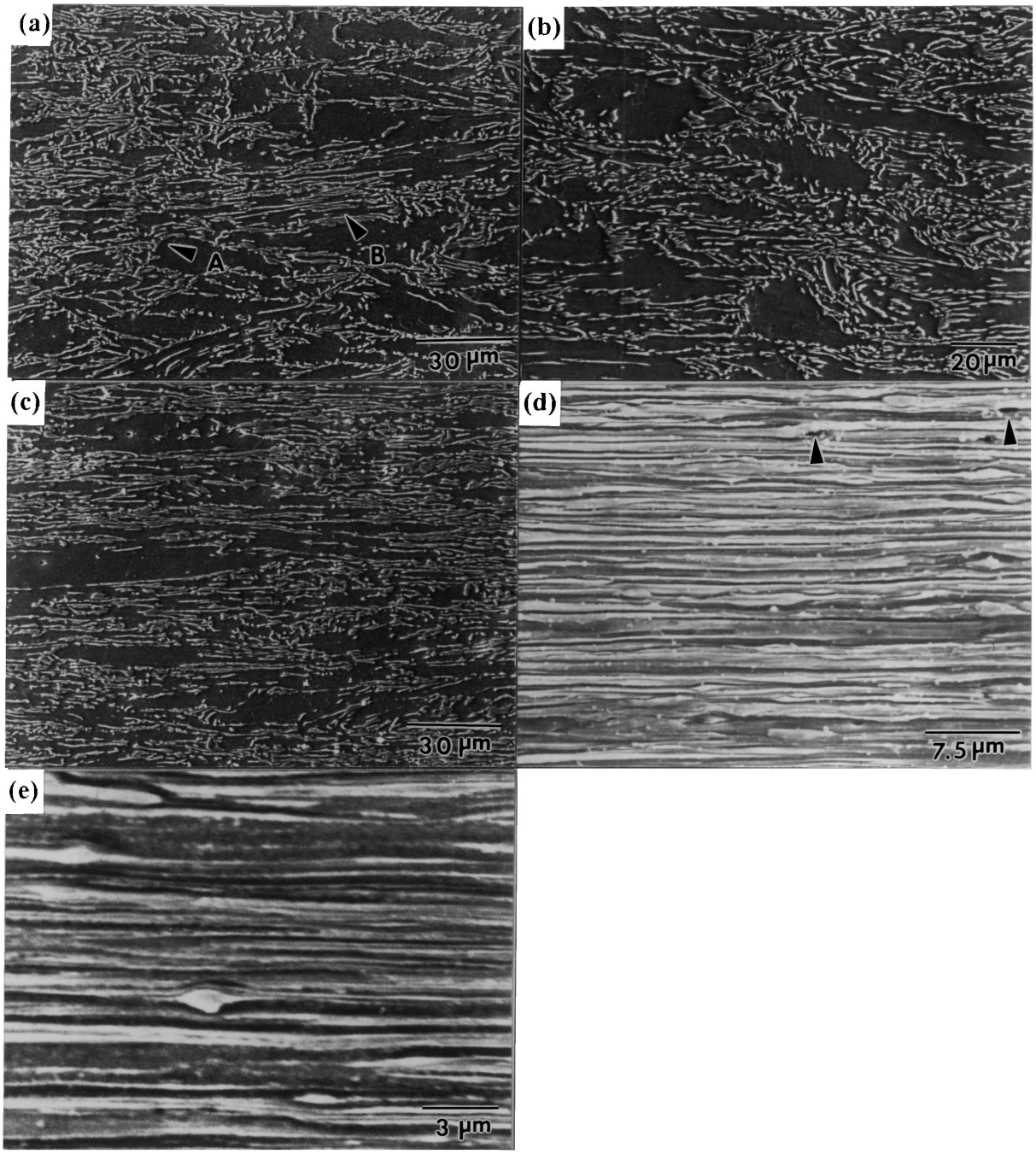

Figure 2 The process of the realignment of martensite particles with the increase of drawing strain in steel A: (a) $\varepsilon = 0.93$; (b) $\varepsilon = 2.04$; (c) $\varepsilon = 2.75$; (d) $\varepsilon = 3.66$; (e) $\varepsilon = 4.48$.

this early stage of deformation. This orientation dependence of deformation behavior can also be observed in pearlitic steels. The main features of microstructural changes in pearlitic steels with increasing strain are a progressive alignment of lamellae along the drawing axis, a reduction of interlamellar spacing, a thinning and necking of cementite lamellae, and void formation [16–21]. However, the process of realignment in dual-phase steels is different from that in pearlitic steels. In dual-phase steels martensite particles themselves must change their orientation in conjunction with the deformation of ferrite grains neighboring martensite particles, while the reorientation process proceeds through the rotation of pearlite colonies in pearlitic steels.

When martensite particles are aligned transverse to the drawing axis, most particles are bent (marked C in Fig. 3a) due to their inherent ductility with low carbon content in the martensite. However, thin martensite which connects initially randomly oriented martensite particles can not endure the applied stress during drawing and fractured (marked D in Fig. 3a), while shear cracking of the martensite occurs in relatively thick particles (marked E in Fig. 3b). In the case of martensite particles aligned nearly parallel to the drawing axis, most particles are thinned (marked F in Fig. 3a) and/or necked (marked G in Fig. 3c). However, when the martensite particle is too thick, fracture occurs in the martensite itself (marked H in Fig. 3d). At low strains below 2.0, in the present investigation, the fracture of martensite does not necessarily nucleate voids as Kim and Thomas reported [22]. From the above results, it is obvious that the deformation behavior of martensite

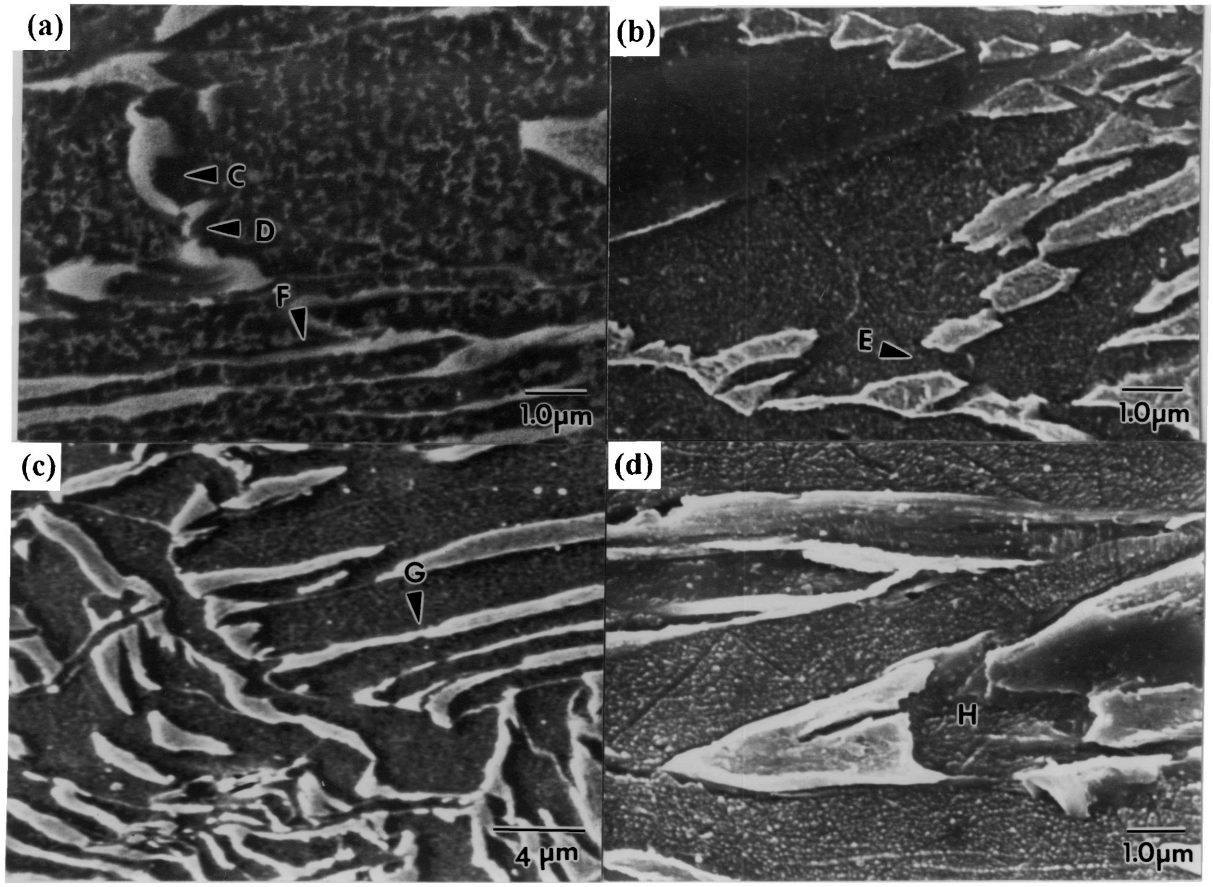

Figure 3 Deformation behavior of martensite particles during drawing: (a) $\varepsilon = 1.08$, steel B; (b) $\varepsilon = 0.82$, steel A; (c) $\varepsilon = 0.93$, steel B; (d) $\varepsilon = 1.64$, steel A.

particles is significantly influenced by their geometry, such as thickness, as well as the stress state imposed by their orientation with respect to the drawing axis. In addition, the interparticle spacing of particles aligned nearly parallel to the drawing axis decreases more rapidly with increasing strain than that of particles aligned transverse to the drawing axis.

The above trends in deformation behavior do not change until most martensite particles are aligned parallel to the drawing axis (Fig. 2). Above a strain of 3.0, most martensite particles are aligned along the drawing axis, and bent martensite particles are rarely found. As shown in Fig. 2d and e, further straining results in the alignment of virtually all martensite particles along the drawing axis and the formation of voids. The formation of voids occurs either by the decohesion of ferrite/martensite interfaces (indicated as arrows in Fig. 2d, marked I in Fig. 4) or by the fracture of martensite deformed plastically (marked J in Fig. 4) during wire drawing. Although, in the present investigation, a quantitative analysis of the void density during drawing has not been performed, the number of voids, i.e., void density, increases as the drawing strain increases. It is interesting to note that these voids did not develope into cracks which cause failure of the wire during drawing. This would be attributed to the healing effect proposed by Porter *et al.* [21] and Avitzur and Avitzur [23]. Porter *et al.* provided evidence of void healing through *in situ* transmission electron microscope (TEM) observation of tensile deformation of pearlitic steel. According to the suggestion by Avitzur and Avitzur, who used the term "self-filling effect", void healing is attributed to the fact that compressive stresses, which are built locally by deformation at the ends of fractured cementite lamellae are enough to close the voids in pearlitic steels. Thus, whether voids develope into cracks or heal depends on the stress state imposed on the voids. If the stress state and geometry of cracks satisfy crack propagation conditions, crack propagation occurs and causes premature failure of the wire during the drawing process. In the present investigation, failure of the wire did not occur until the strain reached about 8.0. Accordingly, it is expected that the voids would rarely developed into cracks in the intermediate strain range,

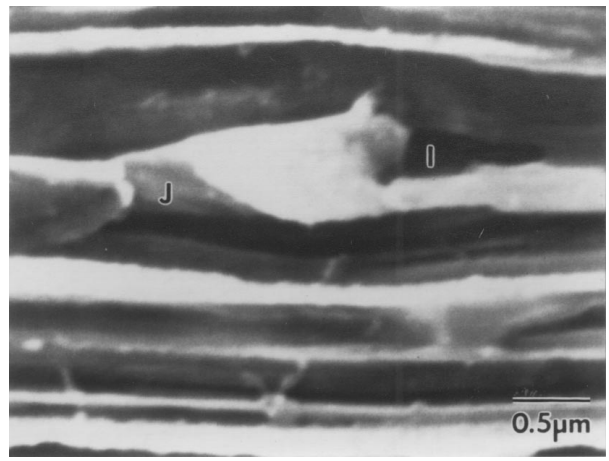

Figure 4 Void formation at martensite particles in steel A ($\varepsilon = 3.66$).

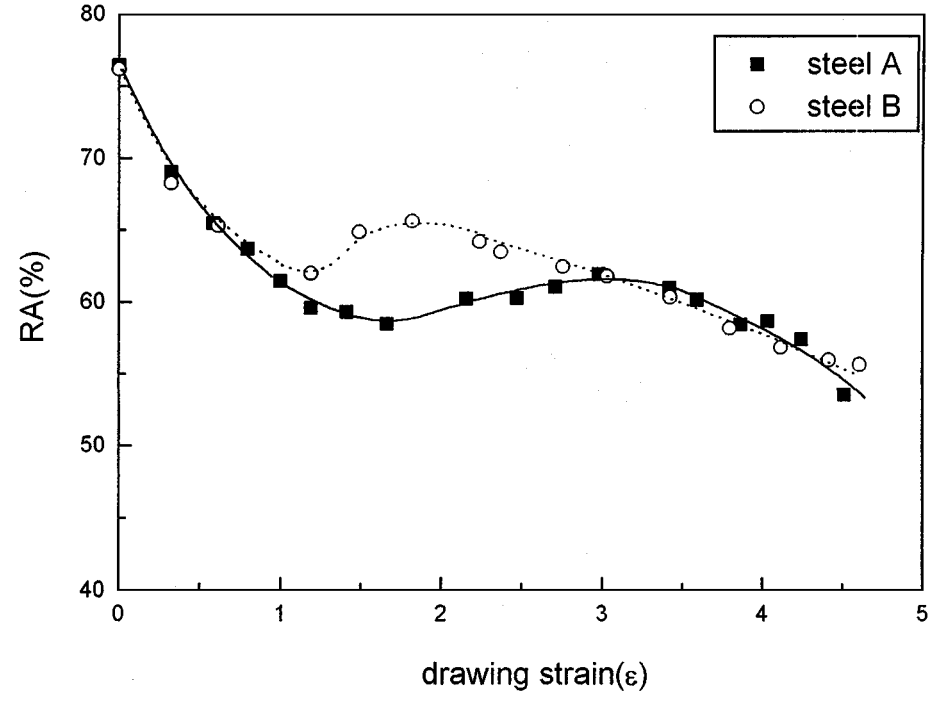

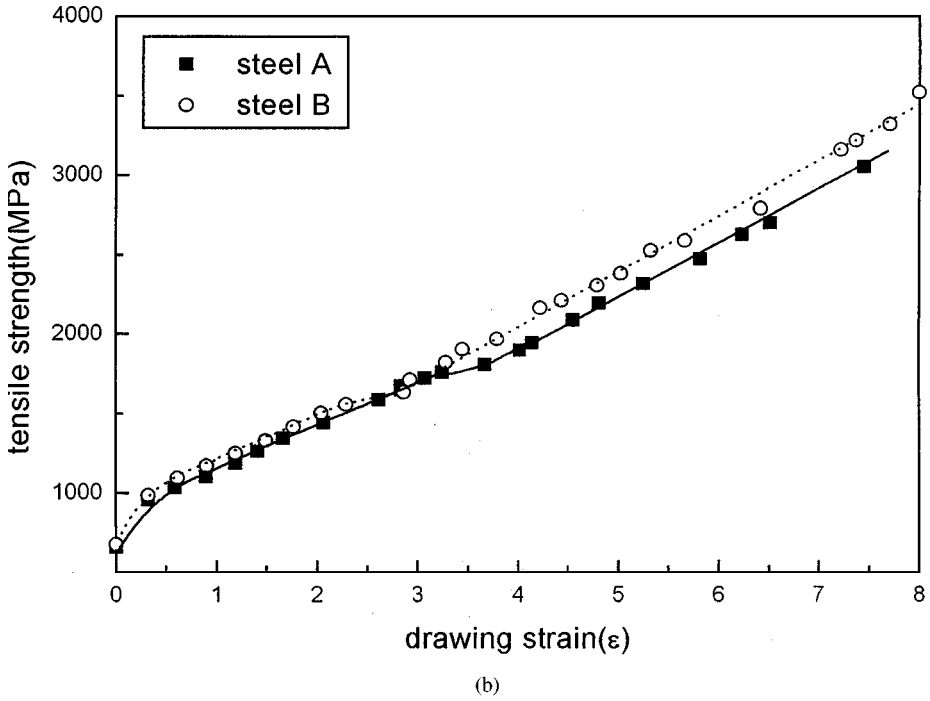

Figure 5 The variations of RA and TS as a function of total strain, ε: (a) reduction in area (RA); (b) tensile strength (TS).

since the voids would be healed or filled with ferrite due to the compressive stress state applied during drawing and the good ductility of the ferrite matrix.

3.2. Variation of mechanical properties

The aforementioned microstructural changes have a close relationship with the variation of mechanical properties in drawn dual-phase wires. The variation of RA and TS are plotted as a function of total strain, ε, in Fig. 5a and b, respectively. RA of the steel wires rapidly decreases, slightly increases and then, gradually decreases after reaching its maximum value with increasing strain. The initial decrease of RA is due to the hardening of the ferrite in the early stage of deformation. The slight increment of RA is attributed to the realignment of randomly oriented martensite particles and the occurrence of a maximum peak of RA would indicate the completion of the alignment of most martensite particles along the drawing axis. The subsequent decrease of RA, after reaching its maximum value, results from the severe deformation of the aligned martensite particles, resulting in thinned, necked and fragmented particles. Fig. 5a shows that the realignment of martensite particles is accomplished at about $\varepsilon = 3.0$ for steel A and $\varepsilon = 2.0$ for steel B. The finer interparticle spacing caused by the larger martensite volume fraction in steel B results in the

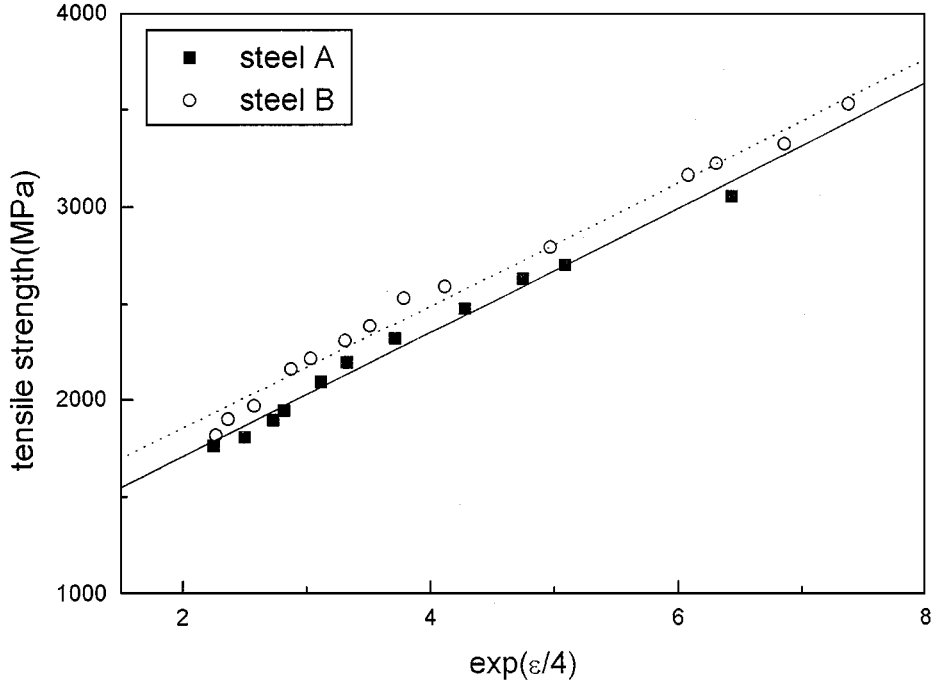

Figure 6 The variation of tensile strength with exp($\varepsilon/4$) at high strains above inflection points.

appearance of a maximum in RA at a lower drawing strain.

Unlike the variation of RA with strain, the tensile strength of the drawn wires increases continuously with increasing the strain, except for inflection points which are related to the accomplishment of the realignment of martensite particles (Fig. 5b). Steel B had a higher tensile strength than steel A. Although the hardness of martensite particles in steel A is a little higher than steel B due to the higher carbon content of the martensite (Table I), the difference is very small. Instead, the decrease of interparticle spacing in steel B contributes to the increase of tensile strength. Thus, the finer interparticle spacing due to the larger martensite volume fraction in steel B results in the higher tensile strength. The influence of interparticle spacing on tensile strength of drawn two-phase materials is well expressed by the Hall-Petch relationship.

$$\sigma = \sigma_0 + K \cdot S^{-1/2} \tag{1}$$

where σ is the tensile strength, σ_0 is the friction stress, K is the Hall-Petch parameter and S is the interparticle spacing. Accordingly, tensile strength continuously increases with drawing strain due to a reduction of interparticle spacing. The fragmentation and the thinning of martensite particles by themselves are not expected to affect work hardening of the wire since martensite acts as an effective barrier against dislocation motion. The rapid increase of tensile strength after the accomplishment of the realignment of martensite particles is attributed to work hardening of the completely aligned fibrous martensite. At high strains above the inflection points where all microconstituents become fibrous, the equation proposed by Embury and Fisher [16] , which is similar in form to the Hall-Petch relationship, is more accurate for expressing the strength of cold drawn steels.

$$\sigma = \sigma_0 + [k_y/(2S_0)^{1/2}] \cdot \exp(\varepsilon/4) \tag{2}$$

where σ is the tensile strength, σ_0 is the friction stress, k_y is the Hall-Petch parameter, S_0 is the initial interlamellar spacing and ε is the drawing strain. Fig. 6 shows a linear relationship of tensile strength with exp($\varepsilon/4$) at high strains above the inflection points. The slopes for drawn wires are 321 and 317 MPa for steel A and steel B, respectively. Although these values are much less than that of cold drawn eutectoid steel wires, about 1000 Mpa, the larger deformable strain (drawing strain without a failure during drawing) of dual-phase steels makes it possible to reach high strength levels.

In Fig. 7, it is shown that the work hardening rate, $\delta\sigma/\delta\varepsilon$, is sensitive to the drawing strain; it rapidly decreases, slightly increases, drops sharply, and then remains constant with increasing the strain. This work hardening rate, $\delta\sigma/\delta\varepsilon$, was determined as the slope at each point of tensile strength in Fig. 5b. The initial decrease of work hardening rate at low strains, which results from work hardening of the ferrite, is commonly observed during tensile testing of dual-phase steels. However, the variations of the work hardening rate above true strain of 1.0, are only observed in drawn two phase bcc materials such as pearlitic steels, which have cementite as a second phase. The variations of work hardening rate at the intermediate strain range (marked as arrows in Fig. 7), i.e., a slight increase and sharp drop, is closely related to the realignment of martensite particles to the drawing axis during drawing. In addition, the existence of the sharp drop indicates the accomplishment of the realignment of martensite particles. After the realignment, both steels show a similar work hardening rate in the high strain range above $\varepsilon = 3.0$.

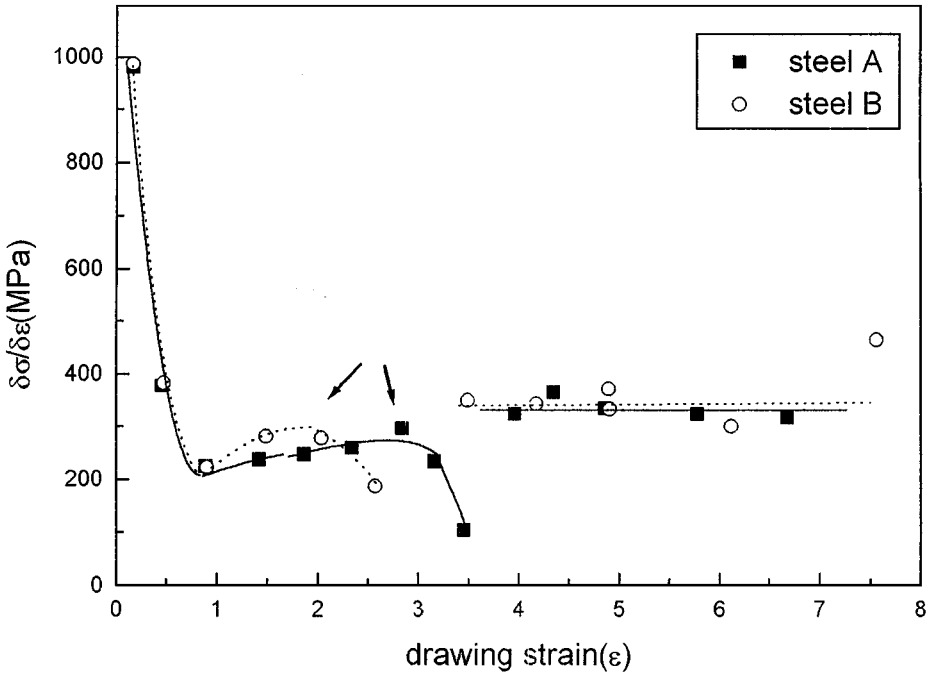

Figure 7 The variation of work hardening rate as a function of drawing strain.

From the above discussion, it is obvious that the variations of mechanical properties such as reduction in area, tensile strength and work hardening rate are closely related to the microstructural evolution during drawing. The realignment of martensite particles to the drawing axis causes the occurrence of a maximum in RA, of an inflection in tensile strength, and of a sharp drop in work hardening rate. Moreover, The finer interparticle spacing caused by the larger martensite volume fraction results in the shift of the maximum in RA to a lower drawing strain and higher tensile strength.

4. Conclusions

From this investigation of microstructural changes during wire drawing and their relationship to mechanical properties in dual-phase steel, the following conclusions were made:

1. Martensite particles aligned nearly parallel to the drawing axis are thinned and necked, while those aligned transverse to the drawing axis are bent or even fractured. In addition, interparticle spacing of particles aligned nearly parallel to the drawing axis decreases more rapidly with increasing strain than that of particles aligned transverse to the drawing axis.

2. The realignment of martensite particles is influenced by the initial interparticle spacing, i.e., martensite volume fraction. The finer interparticle spacing causes the realignment of martensite particles to be accomplished at a lower strain.

3. After the realignment, under the given experimental conditions, although the number of voids increases as the strain increases, the voids rarely develop into cracks in the intermediate strain range less than 8.0, since the voids would be healed or filled with the ferrite.

4. The realignment of martensite particles to the drawing axis is directly related to the occurrence of a maximum in RA, of an inflection in tensile strength and of a sharp drop in work hardening rate.

5. The work hardening rate is sensitive to drawing strain; rapidly decreases, slightly increases, sharply drops, and then remains constant with increasing strain. The variation of work hardening rate is closely related to the microstructural evolution during drawing, as determined by the realignment of martensite particles.

References

1. G. R. SPEICH, in "Fundamentals of Dual-Phase Steels," edited by R. A. Kot and B. L. Bramfitt (TMS-AIME, Warrendale, PA, 1981) p. 3.
2. J. GERBASE, J. D. EMBURY and R. M. HOBBS, in "Structure and Properties of Dual-Phase Steels," edited by R. A. Kot and J. W. Morris (TMS-AIME, Warrendale, PA, 1979) p. 118.
3. M. S. RASHID, in "Formable HSLA and Dual-Phase Steels," edited by A. T. Davenport (TMS-AIME, Warrendale, PA, 1979) p. 1.
4. W. R. CRIBB and J. M. RIGSBEE, in "Structure and Properties of Dual-Phase Steels," edited by R. A. Kot and J. W. Morris (TMS-AIME, Warrendale, PA, 1979) p. 91.
5. D. A. KORZEKWA, D. K. MATLOCK and G. KRAUSS, *Met. Trans. A* **15A** (1984) 1221.
6. T. S. BYUN and I. S. KIM, *J. Mater. Sci.* **28** (1993) 2923.
7. R. G. DAVIES, *Met. Trans. A* **9A** (1978) 41.
8. *Idem., ibid.* **9A** (1978) 671.
9. A. M. SAROSIEK and W. S. OWEN, *Mater. Sci. Eng.* **66** (1984) 13.
10. L. SIDJANIN and S. MIYASATO, *Mater. Sci. & Tech.* **5** (1989) 1200.
11. A. H. NAKAGAWA and G. THOMAS, *Met. Trans. A* **16A** (1985) 831.
12. A. F. SZEWCZYK and J. GURLAND, *ibid.* **13A** (1982) 1821.
13. L. SIDJANIN, S. MIYASATO and G. THOMAS, *Wire Journal Inter.* **12** (1987) 41.
14. F. S. LEPERA, *Metallogr.* **12** (1979) 263.
15. J. J. YI, I. S. KIM and H. S. CHOI, *Met. Trans. A* **16A** (1985) 1237.
16. J. D. EMBURY and R. M. FISHER, *Acta Met.* **14** (1966) 147.
17. J. J. PEPE, *Met. Trans.* **4A** (1973) 2455.

18. M. DOLLAR, I. M. BERNSTEIN and A. W. THOMPSON, *Acta Met.* **36** (1988) 311.
19. M. A. P. DEWEY and G. W. BRIERS, *JISI* **2** (1966) 102.
20. G. LANGFORD, *Met. Trans.* **8A** (1977) 861.
21. D. A. PORTER, K. E. EASTERLING and G. D. W. SMITH, *Acta Met.* **26** (1978) 1405.
22. N. J. KIM and G. THOMAS, *Met. Trans. A* **12A** (1981) 483.
23. B. AVITZUR and B. AVITZUR, *J. Eng. Ind. Trans. ASME Series* **B 92** (1970) 419.

Received 21 May 1997
and accepted 2 March 1999